32ND INTERNATIONAL COSMIC RAY CONFERENCE, BEIJING 2011

Limits on Neutrino Emission from Gamma-Ray Bursts with the 59 String IceCube Detector

THE ICECUBE COLLABORATION[1]
[1]*see special section in these proceedings*

Abstract: IceCube is the first neutrino telescope that has sensitivity to the TeV neutrino flux from GRBs below theoretical predictions and hence is able to put constraints on the model parameters and the cosmic-ray flux from GRBs above 10^{18} eV. The analysis of data from the IceCube 59-string configuration presented here is a dedicated search for neutrinos produced via $p\gamma$-interactions in the prompt phase of the GRB fireball. Yielding no significant excess above the background, the result from this analysis is then combined with the IceCube 40-string configuration result and a stringent limit on the model is set. The combined limit is 0.22 times the predicted neutrino flux. Finally, the implications for the fireball model are discussed.

Corresponding Author: Peter Redl (redlpete@umd.edu), University of Maryland DOI: 10.7529/ICRC2011/V04/0764

Keywords: IceCube, GRB, fireball model, neutrino

1 Introduction

Gamma-ray Bursts (GRBs) are prime candidates for the production of the highest energy cosmic rays because of the enormous energy that is released in such an event [1] ($\mathcal{O}(10^{51} - 10^{54}\mathrm{erg} \times \Omega/4\pi)$ in gamma rays, where Ω is the opening angle of a possible beamed emission). If the prime engine accelerates protons and electrons with similar efficiencies this would be sufficient energy to account for the observed ultra high energy cosmic rays. The observed gamma-rays would originate from high energy electron synchrotron emission and inverse Compton scattering, while high energy neutrons would escape the fireball's magnetic field and later decay to protons, which would be responsible for the high energy cosmic ray flux seen on Earth. The observation of high energy gamma-rays confirms the presence of high energy electrons in the fireball; however, because high energy protons are deflected in inter-galactic and the Galactic magnetic fields no direct observation of protons from GRBs is possible. Nevertheless, if high energy protons are present in the fireball along with high energy electrons it is reasonable to assume that pions will be produced through $p\gamma$ interactions near the source, which would give rise to neutrinos. Guetta et al. [2] gives a detailed account of the expected neutrino flux from such interactions and is the model that is used for the theoretical neutrino prediction in this paper. Previous searches with IceCube and other experiments have given null results, with the most recent search done in IceCube achieving a 90% upper limit that is slightly below the predicted model flux [3]. In this contribution, a further improved limit is presented, which is then combined with the previous one.

2 IceCube

IceCube is a km^3-scale neutrino detector at the South Pole sensitive to TeV-scale neutrinos and above. Construction of the detector finished in December, 2010. IceCube detects Cherenkov light emitted by secondary charged particles produced in neutrino nucleon interactions and uses that information to reconstruct neutrinos. The finished detector is made up of 5160 optical modules (DOMs), with 60 optical modules placed on each of the 86 strings. The results presented here were obtained with the 59-string configuration of IceCube, which took data from 05/20/09 to 05/31/10. IceCube is able to detect all known neutrino flavors; however, in this analysis the focus was on ν_μ. Furthermore, IceCube is sensitive to the entire sky; however, because of the large cosmic-ray muon background in the southern sky, this analysis only considers events that were reconstructed as coming from the northern sky and consequently, only GRBs in that part of the sky were analysed. In this region, the best sensitivity for ν_μ can be achieved in part because of the good angular resolution for muons (0.7° for $E_\nu \gtrsim 10$ TeV) and the low background. The background consists of mis-reconstructed muons (a reducible background) and atmospheric neutrinos (an irreducible background). Both backgrounds have a softer spectrum than the predicted neutrinos from GRBs so event

energy information can be used to improve the signal to background ratio.

3 Event Reconstruction

Events in IceCube are reconstructed by fitting the spatial and temporal Cherenkov light hit pattern observed by the DOMs in a muon event using a maximum likelihood method [4][5]. In the energy range that IceCube is sensitive to, neutrinos have sufficiently high energy for the charged current interaction between the neutrino and the nucleon to be forward and hence the muon and neutrino move in a nearly collinear manner, which enables the determination of the neutrino direction from the reconstructed muon. The shape of the likelihood space near the maximum gives an estimate of the reconstruction error of the fit [6]. In addition to knowing the direction of the neutrino, knowing the energy helps to separate signal from background. The stochastic nature of the muon energy loss in the ice, and the fact that many tracks originate outside of the detector makes it impossible to measure the energy of a muon at the neutrino-interaction point directly. Nevertheless, it is possible to measure the energy loss rate of a muon as it traverses the detector, which is correlated to the energy of the muon inside the detector for energies $\gtrsim$ 1 TeV [7]. The energy resolution achieved in this way is 0.3 to 0.4 in $\log_{10}(E)$.

4 The GRB sample

During the IC59 data taking period, 105 GRBs were observed in the northern sky and reported via the GRB Coordinates Network (GCN) [8]. Of those GRBs 9 had to be removed, because IceCube was not taking physics data. GRB090422 and GRB090423 happened during 59-string test runs before the official start of the IceCube-59 runs and were included in the final GRB list as well, which brings the final catalog to 98 GRBs. The GRB localization is taken from the satellite that has the smallest reported error. The start (T_{start}) and stop (T_{stop}) times are taken by finding the earliest and latest time reported for gamma emission. The fluence, and gamma-ray spectral parameters are taken preferentially from Fermi (GBM), Konus-Wind, Suzaku WAM, and *Swift* in this order. The gamma-ray spectra reported by the satellites were used to calculate the neutrino spectra and flux as outlined in Appendix A of [2]. The neutrino energy spectrum was calculated as a power law with two breaks, with the first break corresponding to the break in the photon spectrum and with the second break corresponding to synchrotron losses of muons and pions (Fig 1). GCN does not always report values for all of the parameters used in the neutrino spectrum calculation. In that case average values are used for the parameters not measured by the satellites. GRBs are classified into two groups: long soft bursts, which are all bursts with a duration longer than 2 seconds and short-hard bursts, which are all bursts with a duration of less than 2 seconds. Average parameters from [3] were used.

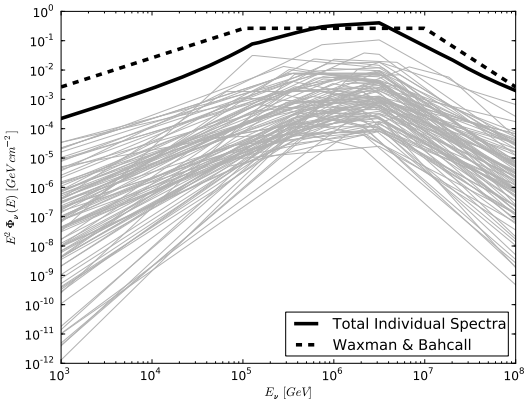

Figure 1: Neutrino spectra of the GRBs used in this analysis. The thin lines represent the individual bursts while the solid thick line represents the sum of all bursts. Finally, the dashed line shows the Waxman 2003 [9] prediction normalized to the number of GRBs observed.

5 Analysis

The analysis presented here was designed to be sensitive to neutrino production from $p\gamma$ interactions in the prompt phase of the fireball. To separate signal from background a Boosted Decision Tree [10] was trained. The analysis was then optimized for discovery with respect to the Boosted Decision Tree score. The optimized value resulted in a final data sample of 85% atmospheric neutrinos and 15% miss-reconstructed cosmic ray muons in the off time data sample (any events not within ± 2 hours of a GRB). An unbinned maximum likelihood search [11] was performed and each event passing the boosted decision tree cut was assigned a probability of being a signal event from a GRB or a background event. The final likelihood is the product of three PDFs based on the location of an event with respect to a GRB, the timing information of the event with respect to the prompt gamma-ray emission, and the energy. The directional signal PDF is a two-dimensional Gaussian:

$$\mathrm{PDF}_i^S(\vec{x}) = \frac{1}{2\pi(\sigma_i^2 + \sigma_{GRB}^2)} e^{\frac{|\vec{x}_i - \vec{x}_{GRB}|^2}{2(\sigma_i^2 + \sigma_{GRB}^2)}} \qquad (1)$$

where σ_i is the directional uncertainty for the i^{th} event and σ_{GRB} is the uncertainty of the GRB location as reported by GCN. $|\vec{x}_i - \vec{x}_{GRB}|$ is the angular difference between the reconstructed muon direction and the GRB location reported by GCN. The background spacial PDF was constructed from off-time data, taking into account the direction-dependent acceptance of the detector.

The time PDF is flat over the duration (T_{100}) of the burst and falls off smoothly as a Gaussian on either side. The

width, σ, of the Gaussian is equal to the T_{100} of the burst with a minimum of 2 s and a maximum of 25 s .

The third component of the likelihood is an energy PDF. In previous analyses, a single energy PDF for the whole northern sky was used [3, 11]. However, because the Earth is opaque to neutrinos above $\sim$ 100 TeV, the northern sky was split into three zenith regions in order to account for this effect. The signal energy PDFs were computed from the reconstructed muon energy-loss (dE/dx) from signal simulation and averaged over all GRBs in a region. The energy background PDF was computed from the dE/dx distributions of all off-time data in each region.

The final likelihood is maximized by varying the assumed number of signal events n_s and a test statistic λ is computed from the likelihood ratio $L(n_s = \hat{n}_s)/L(n_s = 0)$, where $\hat{n}_s$ is the number of signal events for the maximized likelihood. A distribution, λ, for the background-only case is constructed from off-time data by scrambling it in time a sufficient number of times. By comparing the λ value for the on-time data with the background-only distribution a p-value for the measurement is derived, which is a measure for the compatibility of the measurement with the background-only hypothesis.

6 Result

No events were found in the on-time data to be on-source (within 10° of a GRB) and on time with a GRB and the likelihood maximization yielded $\lambda = 0$. In total 24 background events (not necessarily on source) were expected to be in the total time window and 21 were observed (none on-source). From the Guetta et al. model [2] 5.8 signal events were predicted and a final upper limit of 0.46 times the predicted flux can be set. This limit includes a 6% systematic uncertainty. The systematic uncertainty is estimated by varying parameters in the signal simulation and recomputing the limit, with the dominant factor being the efficiency of the DOMs (the uncertainty of the DOM-efficiency is $\sim 10\ \%$).

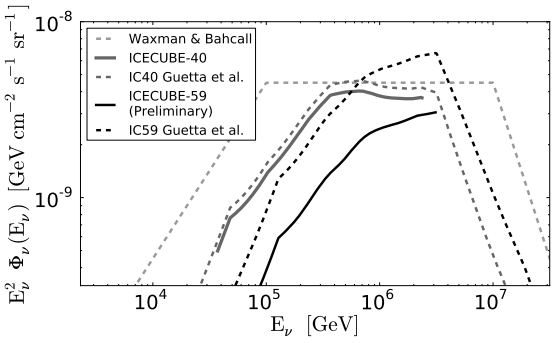

Figure 2: This plot shows the result of this analysis along with the result of the previous analyses. The flux lines from the predictions from Guetta et al. [2] and Waxman 2003 [9] are shown as well.

The corresponding model dependent result presented in a previous analysis [3] sets a limit of 0.82 of the model flux. This limit was obtained using data from the IceCube detector in the 40-string configuration. It is possible to combine this limit with the limit presented in this paper [3], because both analyses obtain a null result. The limits are combined by using signal simulation from each analysis and combining them into one signal simulation data set. From the combined signal data set a new limit is calculated by finding the fraction of total signal flux that would have yielded a *test statistic* that was greater than zero in either analysis in 90% of the cases. This new fractional signal flux is the combined limit and is 0.22 times the flux calculated according to Guetta et al. [2]. Systematic uncertainties were handled by combining the worst limit from each analysis which makes the combined limit conservative with respect to systematic uncertainties. Figure 3 shows the combined limit from these two analyses.

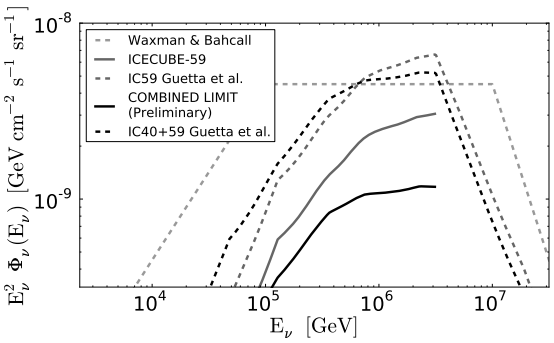

Figure 3: The combined limit of the IC40+59 analysis is shown in addition to the limits and flux predictions displayed in Fig.2.

7 Discussion

Previous results have excluded the neutrino production models outlined in [2] and [9] at a level where it may still have been explained by statistical fluctuations. This analysis is able to exclude the models with high confidence and if the result is combined with the previous result the model in question is strongly disfavored. The caveat is that there are parameters in the model for which average values, or theoretically calculated values are used, because they are not measured (or rarely measured) by the satellites. The bulk Lorentz Factor Γ is one of these values. The lower limit on this value is established by pair production arguments [2], but the upper limit is less clear. Recent papers [12, 13, 14] suggest that Γ can take values of up to 1000 (316 was used in this analysis as well as in [11, 3]). Γ is an important parameter, because in this analysis the GRBs that have the highest neutrino expectation also have the highest energy gamma-rays observed by Fermi's LAT [15]. Because of pair production arguments [2], this indicates higher Γ factors, which implies that the theoretical

brightest GRBs in the neutrino sky would be suppressed in practice. Another unmeasured parameter that could contribute to the non-detection of a neutrino flux from GRBs is the variability of the observed γ-ray light curve, t_{var}. This parameter is assumed to be the characteristic time scale between the collision of different shock fronts in the GRB fireball. Conceptually, if this time is shorter, shock fronts will collide more frequently, causing a greater number of accelerated particles and therefore more neutrinos. Recent limits on t_{var} indicate that if t_{var} is varied by a factor of 10 (either higher or lower) UHECR could still be explained as originating from GRBs [16]. Therefore, t_{var} was varied by a factor of 10 and the limit was recomputed in incremental steps from $0.1 - 10$ times the standard t_{var} value. In Fig. 4 the limit of this analysis is plotted as a function of Γ and t_{var}. It is also useful to ask, how well IceCube will do in

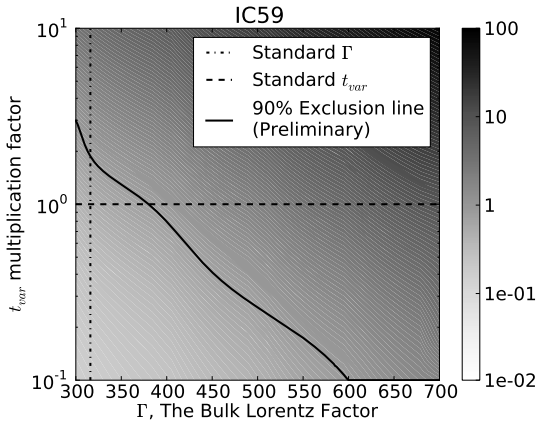

Figure 4: Limit set by the IC59 analysis as a function of the t_{var} multiplication factor and Γ assuming the Guetta et al. model [2]. The gray scale indicates the fraction of the model flux that can be excluded at each point of the phase space at 90% CL. The thick black line indicates where $1\times$ the model can be excluded at 90 % CL, while the dashed lines indicated the standard values used in this analysis. The excluded region is the region found to the left and below the exclusion line.

the 86-string configuration with respect to constraining this parameter space. To get a handle on this the GRB catalog from the 59-string configuration was used to estimate the 86-string sensitivity from Monte Carlo simulations. The result for 3-years of 86-string operation is plotted in Fig. 5. As seen from the plot, 3-years of IceCube-86 can exclude a large portion of the allowed parameter space with the portion that is not excluded being disfavored by theory. The parameters that are treated here are not the only variable parameters in the model that are important to the neutrino flux. However, the above parameters alone could account for the null result seen in IceCube so far. Future observations with the completed IceCube detector will be able to exclude or confirm GRBs as the major sources of UHECR production in a few years.

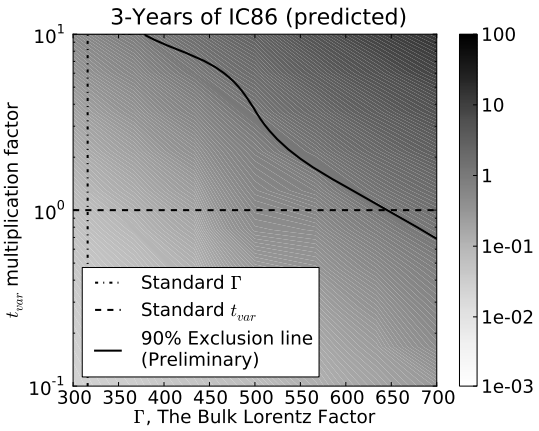

Figure 5: Projected sensitivity of IC86 after 3 years of operation with respect to Γ and t_{var}.

References

[1] E. Waxman. *Phys. Rev. Lett.*, 75:386–389, July 1995.

[2] D. Guetta, D. Hooper, J. Alvarez-Muñiz, F. Halzen, and E. Reuveni. *Astroparticle Physics*, 20:429–455, January 2004.

[3] R. Abbasi et al. *Phys. Rev. Lett.*, 106:141101, 2011.

[4] J. Ahrens, (AMANDA Collaboration), et al. *Nucl. Instrum. and Meth. A*, 524:169–194, May 2004.

[5] N. van Eijndhoven, O. Fadiran, and G. Japaridze. *Astropart. Phys.*, 28:456–462, 2007.

[6] T. Neunhöffer. *Astroparticle Physics*, 25:220–225, April 2006.

[7] Sean Grullon, David Boersma, Gary Hill, Kotoyo Hoshina, and K. Mase. In *Proc. of 30th ICRC, Merida, Mexico*, 2007.

[8] GRB Coordinates Network. `http://gcn.gsfc.nasa.gov`.

[9] E. Waxman. *Nucl. Phys. B Proc. Suppl.*, 118:353–362, April 2003.

[10] Andreas Hoecker, Peter Speckmayer, Joerg Stelzer, Jan Therhaag, Eckhard von Toerne, and Helge Voss. *PoS*, ACAT:040, 2007.

[11] R. Abbasi, (IceCube Collaboration), et al. *ApJ*, 710:346–359, February 2010.

[12] Johan Bregeon et al. *Astrophys. J.*, 729:114, 2011.

[13] En-Wei Liang et al. *Astrophys. J.*, 725:2209–2224, 2010.

[14] Alicia M. Soderberg and Enrico Ramirez-Ruiz. *AIP Conf. Proc.*, 662:172–175, 2003.

[15] NASA. Fermi: Gamma ray space telescope. 2008. `http://fermi.gsfc.nasa.gov/`.

[16] M. Ahlers, M. C. Gonzalez-Garcia, and F. Halzen. *submitted to ApJ*, 2011. arXiv:1105.2326.